Biochemical Pharmacology, Vol. 40, No. 8, pp. 1747–1756, 1990.
Printed in Great Britain.

0006-2952/90 $3.00 + 0.00

METABOLISM OF NICOTINE BY HEPATOCYTES

GABRIEL A. KYEREMATEN,* MONICA MORGAN,* GENEVIEVE WARNER,* LOUIS F. MARTIN† and ELLIOT S. VESELL*‡

Departments of *Pharmacology and †Surgery, The Pennsylvania State University College of Medicine, Hershey, PA 17033, U.S.A.

(*Received* 13 *February* 1990; *accepted* 17 *April* 1990)

Abstract—The profile of nicotine metabolites produced by freshly isolated hepatocytes from rats, hamsters, guinea pigs, mice and humans was investigated after a 30-min exposure to nicotine ([2-^{14}C]pyrrolidine). Large species differences occurred in the extent of nicotine metabolism; these ranged from 95% metabolism in guinea pig hepatocytes to only 30% metabolism in human and rat hepatocytes. The spectrum of metabolites formed also varied widely in different species. In hepatocytes from obese human subjects, nicotine was metabolized most extensively in smokers, least in nonsmokers, and to an intermediate degree in exsmokers, suggesting that cigarette smoking enhances the rate of nicotine metabolism. Pretreatment of all nonhuman species studied with phenobarbital and β-naphthoflavone and with Aroclor in rats produced distinctive inductive patterns. Phenobarbital pretreatment of nonsmokers for 2 days prior to liver biopsy doubled the extent of nicotine conversion to cotinine by their hepatocytes. Rat and hamster hepatocytes exhibited sex and stereoselectivity differences in nicotine metabolism. Collectively, these studies indicate that hepatocytes offer some advantages over *in vivo* systems in investigating certain aspects of nicotine metabolism.

This study was designed to establish the pattern of nicotine metabolism in hepatocytes from rats, hamsters, guinea pigs, mice and humans. In particular, we asked how closely hepatocytes maintained certain characteristics of nicotine metabolism identified *in vivo*, including species and sex differences [1–4], induction profile [5–7] and stereoselectivity [2, 3, 8].

The advantage of hepatocytes resides in their potential for reflecting subtle metabolic changes concealed *in vivo* when such alterations are offset by simultaneously occurring changes in rates of drug absorption, distribution and excretion. For example, in humans [9] and rats [1] differences in the rates of nicotine metabolism were balanced by concurrent changes in nicotine volume of distribution. A reliable *in vitro* experimental model, unaffected by *in vivo* absorption and distribution factors, could prove useful in delineating small, but nonetheless important, changes that may occur in intrinsic nicotine metabolism.

Several *in vitro* systems, including crude/purified microsomal preparations [10, 11], liver slices [12, 13] and a perfused liver system [7], have already served to elucidate the complex pathways of nicotine metabolism. Hepatocytes, on the other hand, while used previously with respect to conversion of nicotine to cotinine [14], have not been evaluated for the complete profile of nicotine metabolism. As intact cell systems, hepatocytes retain most metabolic capabilities of liver, while allowing, under well defined, carefully controlled conditions, examination of effects produced by various manipulations. Hepatocytes thus provide unique opportunities to study mechanisms and pathways of drug metabolism in different species, including humans [15]. Since metabolism of many drugs in hepatocytes correlates closely with their metabolic profile *in vivo* [15–17], we decided to evaluate how well freshly isolated hepatocytes could serve as an experimental model for nicotine metabolism. Nicotine metabolism is appropriate for such an approach because it is complex [18], and several pathways are subject to environmental pertubations [6].

‡ Correspondence: Elliot S. Vesell, M.D., Department of Pharmacology, The Pennsylvania State University, College of Medicine, P.O. Box 850, Hershey, PA 17033.

MATERIALS AND METHODS

Materials. Racemic (*R*)-(+)/(*S*)-(−)-nicotine ([2-^{14}C]pyrrolidine), stored in ethanol under argon, was obtained from New England Nuclear (Boston, MA) and had specific activity of 60 mCi/mmol. Unlabeled (*S*)-(−)- and (*R*)-(+)-nicotine were purchased from the Sigma Chemical Co. (St. Louis, MO). The (*R*)-(+)-entaniomer was obtained as the (+)-di-*p*-toluoyltartrate salt. Sodium chloride, potassium chloride, magnesium sulfate, sodium phosphate dibasic, potassium phosphate monobasic and sodium acetate were purchased from Fisher Scientific (Pittsburgh, PA). Calcium chloride and HPLC grade methanol and acetonitrile were purchased from the J. T. Baker Co. (Phillipsburg, NJ). Bovine serum albumin (fraction V), EDTA, collagenase (type IV), trypan blue and NADPH were obtained from the Sigma Chemical Co. and Tris–KCl from Schwarz/Mann Biotech (Cleveland, OH). The inducing agents, phenobarbital (sodium salt), β-naphthoflavone, Aroclor 1254 and 3-methylcholanthrene, were purchased, respectively, from Merck & Co., Inc. (Rahway, NJ); Aldrich Chemical Co., Inc. (Milwaukee, WI); Chem Service (West Chester, PA); and Eastman Kodak Co. (Rochester, NY).

Animals. Adult male Sprague–Dawley (Crl:SD) rats (100–120 g) and Syrian (Crl:LVG) hamsters (80–100 g) were purchased from Charles River

Breeding Laboratories (Wilmington, MA). Adult male Hartley (Hra) guinea pigs (200–250 g) were from Hazleton Research Animals (Denver, PA). Adult male DBA/Jax mice (20–25 g) were purchased from Jackson Laboratories (Bar Harbor, ME). All animals were kept under observation in our quarantine facilities for 1 week before the study. They were housed four to a cage in a temperature-controlled environment (22° ± 1°). The relative humidity varied between 40 and 60%; a 100% exchange of fresh air was accomplished 18–22 times every hour. The photoperiod was controlled to provide light from 8:00 a.m. to 8:00 p.m. Animals received water and a close-formula, cereal-based diet (Ralston-Purina) *ad lib.*

Wedges of human hepatic tissue were obtained with signed informed consent from 27 grossly obese male (7) and female (20) patients undergoing scheduled liver biopsy prior to a surgical procedure termed gastroplasty performed at this institution. The medical background of each patient, including tobacco smoking history, was recorded carefully. Subjects who denied using tobacco were classified as nonsmokers. Smokers had consumed at least one pack of cigarettes a day over the previous year, and exsmokers had stopped smoking at least 3 months prior to the study.

Induction protocol. Phenobarbital (70 mg/kg) was administered intraperitoneally once daily for 3 days. β-Naphthoflavone, 3-methylcholanthrene and Aroclor 1254 were injected intraperitoneally in single doses of 40, 80 and 300 mg/kg respectively. Phenobarbital-, β-naphthoflavone- and Aroclor-administered animals were killed 96 hr following start of pretreatment, whereas 3-methylcholanthrene-pretreated animals were killed after 72 hr. Phenobarbital was dissolved in physiological saline adjusted to pH 8.5. The other inducing agents were solubilized in peanut oil. Appropriate doses of these vehicles, saline and peanut oil, were administered to control groups of animals. In human subjects, phenobarbital (100 mg, po) was given at bedtime for 2 days before surgery.

Preparation of hepatocytes. Rat, hamster and guinea pig hepatocytes were isolated according to a modification of the EDTA method of Wang *et al.* [19]. Briefly, the animal was anesthetized with ether and the portal vein cannulated for liver perfusion. A 17-gauge needle was used for rats/guinea pigs, whereas hamsters were cannulated with a 20-gauge needle. Perfusion was started *in situ* with buffer A which consisted of NaCl (140 mM), KCl (5 mM), $MgSO_4$ (1.6 mM), KH_2PO_4 (0.4 mM), EDTA (2.0 mM), $NaHCO_3$ (25 mM), pH 7.4. Buffer A was maintained at 37° and equilibrated with O_2:CO_2 (95:5, v/v). With the cannula in place, the liver was excised by first removing the ventricle and intestine in one piece followed by its liberation from the diaphragm and, finally, with the rat in a tilted position, by cutting the dorsal ligaments. The freed liver was immersed in a liver perfusion system [20], and perfusion continued with buffer A for a total of 30 min. To loosen cells, the swollen liver was rinsed and diced in buffer B (same composition as buffer A except 1.0 mM $CaCl_2$ replaced EDTA). The cell suspension was strained through two layers of gauze and centrifuged at 2000 *g* for 2.5 min. The cell pellet was then washed twice with buffer B and after the final wash, suspended in buffer C (buffer B with bovine serum albumin, 2%). Cell viability and count were estimated by the trypan blue exclusion test [20]. At room temperature, a 2% aqueous trypan blue solution was mixed with an equal volume of cell suspension diluted 4-fold with buffer C. Viable hepatocytes excluding the dye within 2 min were counted with a hemocytometer.

Mouse and human hepatocytes were isolated by the two-step collagenase perfusion procedure [20] in order to obtain cell yields comparable to those obtained from hamsters, guinea pigs and rats using the EDTA method. Cannulation of the hepatic portal vein of mice was accomplished utilizing a 22-gauge needle, whereas human liver biopsy wedge samples were perfused according to the method of Strom *et al.* [21]. Buffer A was perfused initially for 6 min and followed with collagenase (0.12% in buffer B) for 9 min. Subsequent processing of perfused human and mouse livers was as described above for hamsters, guinea pigs and rats.

Measurement of nicotine metabolism. The incubation mixture for nicotine metabolism consisted of the following: nicotine ([2-^{14}C]pyrrolidine), 0.1 μCi; unlabeled nicotine, 0.01 mM; NADPH, 0.5 mM; Tris–KCl (pH 7.4), 100 mM. This mixture had a final volume of 500 μL and was brought to 1 mL when the reaction was initiated by adding 500 μL of hepatocyte

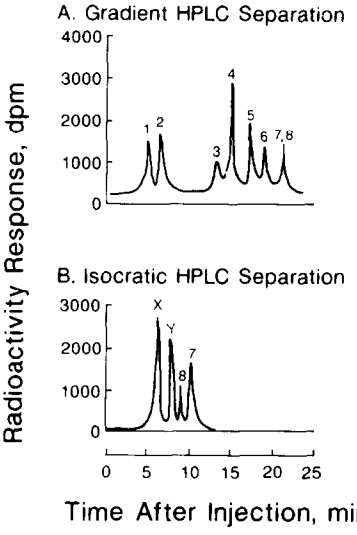

Fig. 1. HPLC separation of nicotine and metabolites extracted from hamster hepatocyte suspensions following a 30-min incubation with [^{14}C]nicotine. Injection volume was 100 μL. The upper panel (A) shows separation of nicotine (7) from allohydroxydemethylcotinine (1), cotinine-*N*-oxide (2), γ-(3-pyridyl)-γ-oxo-*N*-methylbutyramide (3), 3-hydroxycotinine (4), cotinine (5), nornicotine (6) and nicotine-1′-*N*-oxide (8) using the binary gradient HPLC procedure described in Materials and Methods. The lower panel (B) illustrates separation of nicotine-1′-*N*-oxide (8) from nicotine (7), using the isocratic HPLC method we developed specifically for assay of nicotine-1′-*N*-oxide formation by hepatocytes.

suspension diluted to contain 5.0×10^6 cells/mL. Incubations were carried out under aerobic conditions (O_2:CO_2; 95:5, v/v) at 37° for 30 min in a Dubnoff metabolic shaking incubator. These reaction conditions were determined to be optimum (see Fig. 2A–D). Reactions were terminated by addition of 2 mL of ice-cold methanol. After removal of coagulated proteins by centrifugation, the supernatant fraction was concentrated to a 720 μL volume under a steady stream of nitrogen at 45°. A 100-μL aliquot of the concentrate was injected into the HPLC system to analyze nicotine metabolite production.

HPLC conditions. HPLC analysis was performed on a Waters (Bedford, MA) liquid chromatographic system comprised of a WISP 710B autosampler, two M510 solvent delivery systems controlled by an M680 automated gradient controller and an M440 absorbance detector. Absorbance at 254 nm was monitored on a Chromatopac C-R3A data processor (Shimadzu, Columbia, MO). Radioactivity in the HPLC effluent was monitored with an LB505 Berthold radioactivity monitor system (Berthold Analytical, Nashua, NH) using a 400-μL polytetrafluroethylene flow cell packed with G glass scintillator beads for heterogenous counting. The radioactivity signal was stored and integrated by an LB510 Berthold chromatography data station. The analytical column was a 150 × 4.5 mm, 5 μm IBM Optima cyano RP cartridge (IBM Instruments, Danbury, CT) which was connected in series with and preceded a 250 × 4.5 mm, 5 μM IBM cyano RP analytical steel column. A 50 × 4.5 mm, 5 μm IBM Optima cyano RP cartridge served as guard column. Two solvent systems, designated A and B, comprised the mobile phase. Solvent A was water/methanol/

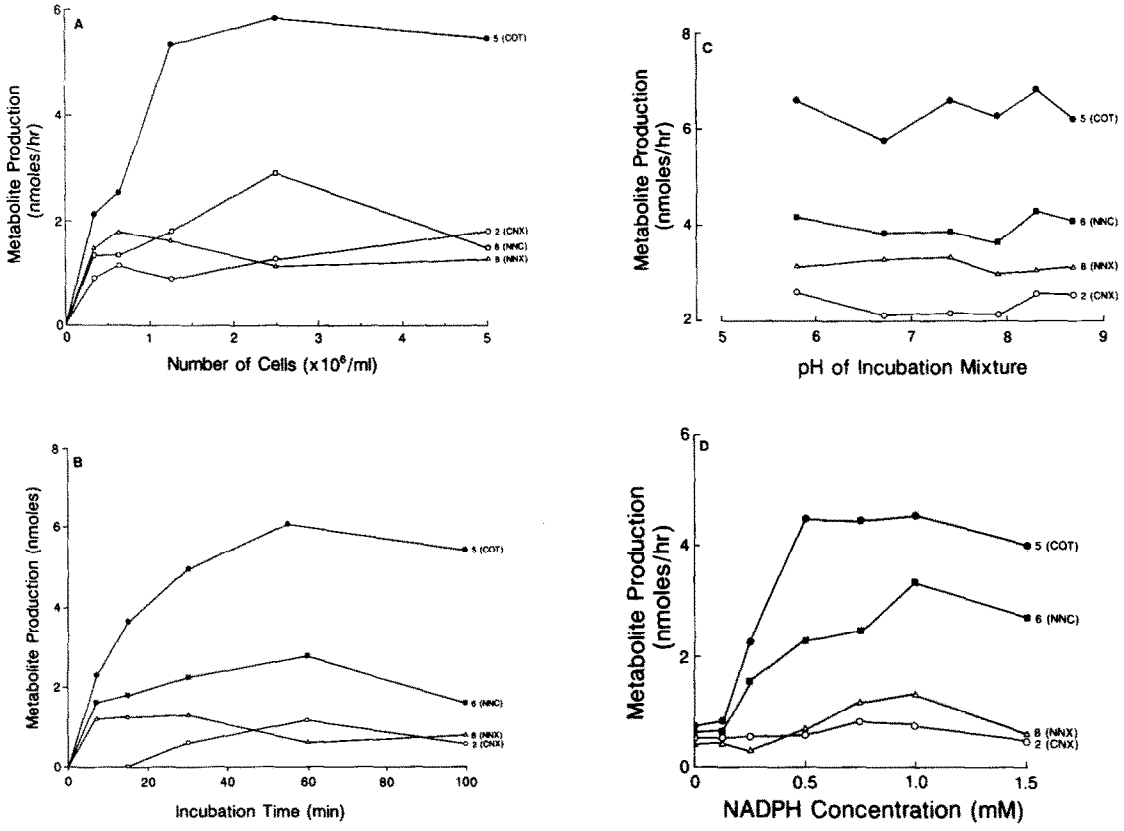

Fig. 2. (A) Effect of hepatocyte number on nicotine metabolism in phenobarbital-induced Sprague–Dawley rats. The reaction mixture consisted of nicotine ([2-^{14}C]pyrrolidine), 0.1 μCi; *S*-(−)-nicotine (unlabeled), 0.01 nM; NADPH, 0.5 mM; Tris–KCl (pH 7.4), 100 mM. Incubations were carried out at 37° for 30 min. Key: COT, cotinine; NNC, nornicotine; NNX, nicotine-1′-*N*-oxide; and CNX, cotinine-*N*-oxide. Numbers at the end of each line correspond to the numbers above each peak in Fig. 1. (B) Time-courses of nicotine metabolite production by hepatocytes isolated from phenobarbital-induced Sprague–Dawley rats. The reaction mixture consisted of: nicotine ([2-^{14}C]pyrrolidine), 0.1 μCi; *S*-(−)-nicotine, 0.01 mM; NADPH, 0.5 mM; Tris–KCl (pH 7.4), 100 mM; hepatocyte suspension, containing 2.5×10^6 cells. (C) Effect of pH of incubation mixture on nicotine metabolite production by hepatocytes isolated from phenobarbital-induced male Sprague–Dawley rats. The reaction mixture consisted of: nicotine ([2-^{14}C]pyrrolidine), 0.1 μCi; *S*-(−)-nicotine, 0.01 mM; NADPH, 0.5 mM; Tris–KCl, 100 mM; hepatocyte suspension, containing 2.5×10^6 cells. (D) NADPH dependence of nicotine metabolite production by hepatocytes isolated from phenobarbital-induced male Sprague–Dawley rats. The reaction mixture consisted of: nicotine ([2-^{14}C]pyrrolidine), 0.1 μCi; *S*-(−)-nicotine, 0.01 mM; Tris–KCl (pH 7.4), 100 mM; hepatocyte suspension, containing 2.5×10^6 cells. For each panel, N = 6.

0.1 M acetate buffer (pH 4.0)/acetronitrile (187.5:11:1:0.5, by vol.) and solvent B was water/methanol/0.5 M acetate buffer (pH 4.0)/acetonitrile (65:29:4:2, by vol.) which was adjusted to pH 6.82 with triethylamine. A binary gradient system, which consisted of a mixture of solvents A and B (99:1, v/v) as system 1 and solvent B as system 2, was used to separate nicotine and its *in vitro* metabolites. The gradient program consisted of an initial 5-min run of system 1, followed by a 10-min gradient ascent (Curve No. 8 on Waters M680 gradient controller) to system 1/system 2, 50:50 which was then maintained for 5 min. Initial conditions were then re-established by equilibrating the column with 100% system 1 for 20 min. The solvent flow rate was 1.5 mL/min throughout the 40-min run.

This HPLC method separates nicotine (NIC) from six of its metabolites—allohydroxydemethylcotinine (ADC), cotinine-*N*-oxide (CNX), γ-(3-pyridyl)-γ-oxo-*N*-methylbutyramide (POMB), 3-hydroxycotinine (3HC), cotinine (COT) and nornicotine (NNC). Under these conditions, however, a seventh metabolite, nicotine-1′-*N*-oxide (NNX), is inadequately resolved from nicotine, thereby necessitating development of a separate assay for it. Separation of nicotine-1′-*N*-oxide from nicotine was achieved with solvent B run isocratically on the same HPLC column at a flow rate of 1.5 mL/min.

Data analysis. For each assay, we calculated the percent contribution of each metabolite formed and of unmetabolized nicotine to the total radioactivity present in the starting nicotine. Differences between means of these calculated percentages were tested for statistical significance using Student's *t*-test for unpaired data.

RESULTS

HPLC fractionation. Figure 1A shows the HPLC separation pattern for nicotine and six metabolites produced by hamster hapatocytes incubated with [^{14}C]nicotine. For this separation, we used the binary gradient system described earlier. Figure 1B shows on the same column, but under isocratic conditions, separation of the seventh metabolite, nicotine-1′-*N*-oxide from nicotine. Peaks designated X and Y are cotinine and nornicotine, respectively, but contain additional metabolites (1–4 in Fig. 1A) not readily separable by the simpler isocratic method.

Pre-HPLC recovery of nicotine and metabolites, estimated from total dpm in extracts prior to HPLC injection, was 91.7 ± 1.6%.

Optimization of conditions for nicotine metabolism. The effects of four "incubation" factors on nicotine metabolite production are illustrated in Fig. 2A–D. Hepatocytes used in this study were isolated from phenobarbital-pretreated rats. The factors monitored were hepatocyte number, period of incubation, pH and NADPH concentration of incubation mixture. Hepatocyte counts of 2.5×10^6 cells/mL incubation mixture were the optimum cell number for production of most nicotine metabolites (Fig. 2A). Although maximum production of metabolites occurred within 1 hr (Fig. 2B), we choose for our assays a 30-min incubation period in order to standardize most efficiently variations in loss of hepatocyte viability with time. Clearly, at 30 min, production of most metabolites plateaued so that measurements at this time do not reflect initial rates. Nicotine metabolism did not vary much over the practical pH range of 5.8 to 7.8 (Fig. 2C); thus, we maintained our incubation mixtures at physiological pH, 7.4. Metabolism of nicotine by hepatocytes did require NADPH supplementation (Fig. 2D); an NADPH concentration of 0.5 mM was selected as optimum for metabolite production.

Species and sex differences. Hepatocytes isolated from nonmedicated rats, hamsters, guinea pigs, mice and human subjects exhibited marked variations, both qualitative and quantitative, in their metabolism of nicotine (Figs. 3 and 4; Tables 1–3). Hamster hepatocytes exhibited the most interesting metabolic profile, producing as many as seven nicotine metabolites—allohydroxydemethylcotinine, cotinine-*N*-oxide, γ-(3-pyridyl)-γ-oxo-*N*-methylbutyramide, 3-hydroxycotinine, cotinine, nornicotine and nicotine-1′-*N*-oxide (Fig. 3). Four of these, 3-hydroxycotinine, cotinine, nornicotine and nicotine-1′-*N*-oxide, were extracted from incubations with guinea pig hepatocytes (Fig. 3). In rat and mouse hepatocytes allohydroxydemethylcotinine, cotinine, nornicotine and nicotine-1′-*N*-oxide were recovered in rather low amounts. Following phenobarbital pretreatment, however, these metabolites were produced in appreciable amounts; rat hepatocytes produced cotinine-*N*-oxide as well (Fig. 3). Hepatocytes isolated from most human liver biopsy samples produced only cotinine and nicotine-1′-*N*-oxide (Fig. 3).

Quantitatively, from the percent contribution of unmetabolized nicotine to the total (metabolites plus remaining nicotine), guinea pig and hamster hepatocytes metabolized nicotine to the greatest extent (Fig. 4). The nicotine-metabolizing capacity of guinea pig and hamster hepatocytes did not differ significantly from each other but both were significantly greater than that of mouse, rat and human hepatocytes (Tables 1–3). Nicotine biotransformation tended to be least with rat and human hepatocytes (Fig. 4). High cotinine and nicotine-1′-*N*-oxide production by guinea pig hepatocytes corroborates their high nicotine-metabolizing capacity (Fig. 4; Table 3). These primary metabolites of nicotine were detected only in low concentration in hamster hepatocytes, apparently because they were further biotransformed to more secondary metabolites (Fig. 3; Table 3). Cotinine production was appreciable with mouse and human hepatocytes, but was not significantly greater than that produced by rat hepatocytes. Percent nicotine-1′-*N*-oxide production was similar in incubations with hepatocytes from hamster, mouse, rat and human subjects (Fig. 4).

No sex differences occurred either in the metabolite profile or in the relative percentages of unmetabolized nicotine and of cotinine and nicotine-1′-*N*-oxide produced by hepatocytes from nonmedicated male and female rats (Fig. 4; Table 2).

Induction profile. In studies with human hepatocytes, both cigarette smoking for at least 1 year and phenobarbital pretreatment for 2 days prior to

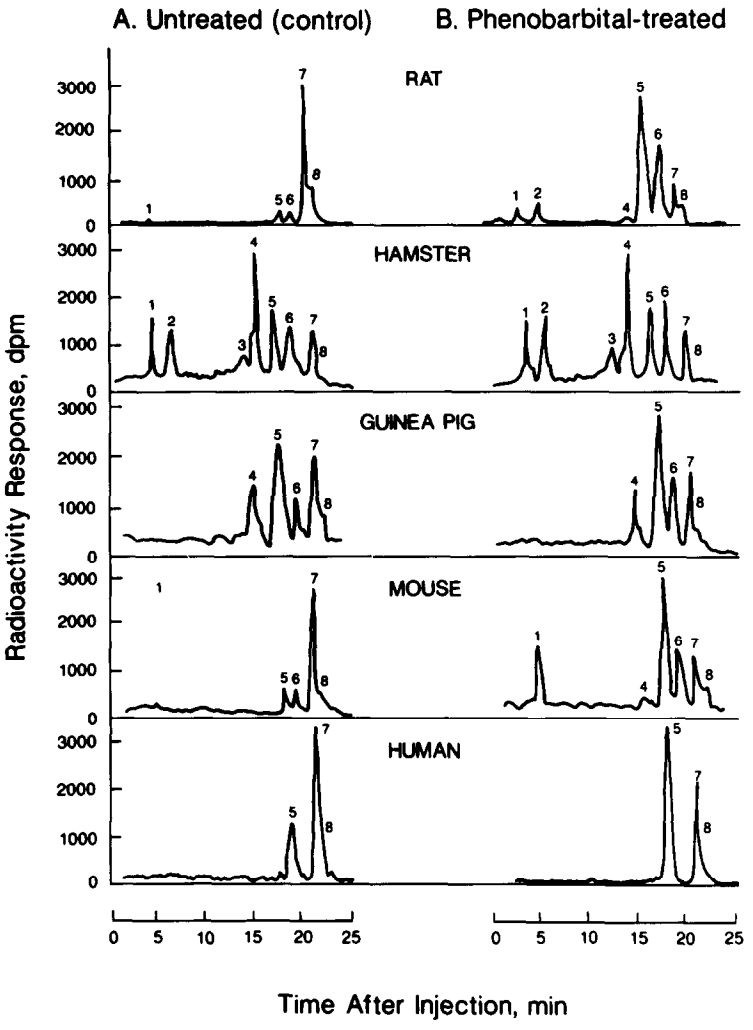

Fig. 3. Species differences in nicotine metabolite production by hepatocytes isolated from (A) untreated (control) and (B) phenobarbital-treated rats, hamsters, guinea pigs, mice and humans. The reaction mixture consisted of: nicotine ([2-^{14}C]pyrrolidine), 0.1 μCi; *S*-(−)-nicotine, 0.01 mM; Tris–KCl (pH 7.4), 100 mM; NADPH, 0.5 mM; hepatocyte suspension, containing 2.5 × 10^6 cells. See legend of Fig. 1 for number key.

biopsy were each associated with significant induction of nicotine metabolism to cotinine (Table 1). A trend toward such induction was also observed with hepatocytes from exsmokers, although differences in cotinine/nicotine recovery between this group and unmedicated nonsmokers did not attain statistical significance. Nicotine-1′-*N*-oxide production by hepatocytes was not affected by either cigarette smoking or phenobarbital pretreatment (Table 1).

In both male and female rats, phenobarbital pretreatment induced nicotine metabolism to cotinine and nornicotine but not to nicotine-1′-*N*-oxide (Table 2). This inductive effect was sex-dependent, being more pronounced in male rats. β-Naphthoflavone and Aroclor 1254 both induced nicotine metabolism in male rats as reflected by the percent ratio of unmetabolized nicotine to the total (Table 2). Whereas cotinine and nornicotine production were enhanced upon Aroclor pretreatment, β-naphthoflavone induced the production of nornicotine and nicotine-1′-*N*-oxide, but not of cotinine (Table 2). Aroclor pretreatment tended to induce nicotine-1′-*N*-oxide production (Table 2).

In hamsters, neither phenobarbital nor β-naphthoflavone enhanced nicotine biotransformation to any of the seven metabolites identified (Table 3). By contrast, in guinea pigs phenobarbital induced the production of 3-hydroxycotinine, cotinine and nornicotine while inhibiting nicotine-1′-*N*-oxide formation (Table 3). β-Naphthoflavone pretreatment apparently had no effect on nicotine metabolism by guinea pig hepatocytes (Table 3); in mice, however, it selectively induced nicotine metabolism to 3-hydroxycotinine, nicotine-1′-*N*-oxide and probably cotinine (Table 3). Nicotine metabolism to 3-hydroxycotinine and cotinine was enhanced in mice upon pretreatment with phenobarbital (Table 3).

Comparative metabolism of nicotine enantiomers. Hamster hepatocytes on exposure to *S*-(−) and *R*-(+)-nicotine exhibited stereoselective biotransform-

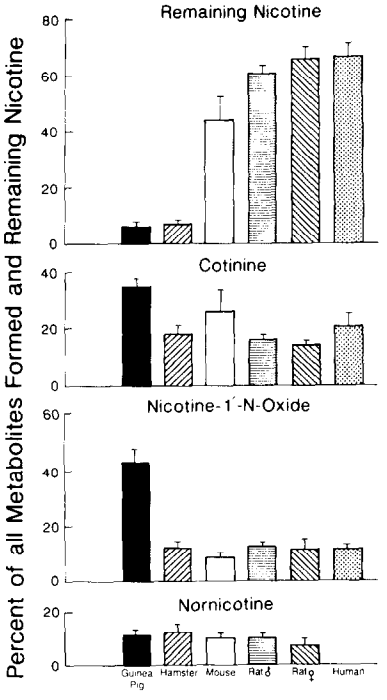

Fig. 4. Metabolism of nicotine in five species arranged in order from the species with the most metabolism (guinea pig) at left to the species with the least metabolism (rat and human) at right. Values indicated are percent contribution ± SE of remaining nicotine and of metabolites formed to the total starting radioactivity; N = 6 in each species except humans where N = 27.

ation of these enantiomers to cotinine and nornicotine (Fig. 5). V_{max} for cotinine production was faster with the *S*-(−)-enantiomer (0.50 ng/hr) than with the *R*-(+)-enantiomer (0.43 ng/hr). With nornicotine production, however, V_{max} for formation from the *R*-(+)-enantiomer (0.22 ng/hr) was faster than that from the *S*-(−)-enantiomer (0.10 ng/hr).

DISCUSSION

These studies define for hepatocytes a complex, species-specific pattern of metabolites formed from nicotine. In rats, this metabolic pattern closely resembles that obtained *in vivo* [18]; the principal metabolites of nicotine observed *in vivo* could be identified in rat hepatocytes. Those few metabolites not observed in hepatocytes occurred in very low concentrations *in vivo* [18]. Due to their limited viability, hepatocytes were studied for only 30 min after nicotine exposure, whereas the *in vivo* investigations were performed after much longer periods (12–96 hr).

Since the present study describes the use of hepatocytes as a new approach to the investigation of nicotine metabolism, its advantages as well as limitations merit consideration. The extreme toxicity of nicotine poses severe limitations for investigations conducted *in vivo*. By contrast, nontoxic nicotine concentrations can readily be used in hepatocytes. Accordingly, the hepatocyte model allows detailed examination of numerous environmental effects on individual pathways of nicotine metabolism. Also, large numbers of cells can be harvested from a single liver, permitting many such studies on genetically identical material, as well as the same pool of enzymes.

The principal disadvantage of the freshly isolated hepatocyte model is the significant loss of cell viability that occurs with time. A second disadvantage involves the difficulties inherent in obtaining human donors [22]. Thus, in the present study only grossly obese donors could be found; results obtained with them may differ from those in normal human subjects.

Large qualitative and quantitative species differences occurred in nicotine metabolism by hepatocytes isolated from five vertebrate species. Hamsters had previously been recognized [23] as a good model for demonstrating nicotine metabolism *in vivo*. Our results disclosed that hamster hepatocytes yielded the most nicotine metabolites (Fig. 3), although the other four species used also produced an array of species-specific nicotine metabolites (Fig. 3).

Table 1. Nicotine metabolism in hepatocytes of smokers, exsmokers and nonsmokers*

	Mean age ± SE	Control		
		COT	NNX	NIC
Nonsmokers (N = 7)	37.9 ± 2.8	20.6 ± 5.7	12.3 ± 1.5	67.1 ± 5.0
Exsmokers (N = 3)	53.3 ± 0.9	25.8 ± 3.8	13.6 ± 5.1	60.6 ± 7.3
Smokers (N = 4)	37.3 ± 4.8	39.4 ± 3.4†	9.4 ± 0.7	51.3 ± 2.9†
	Mean age ± SE	Phenobarbital-treated		
		COT	NNX	NIC
Nonsmokers (N = 5)	40.4 ± 4.4	40.7 ± 6.3‡	11.7 ± 1.8	47.6 ± 5.9‡
Exsmokers (N = 3)	37.3 ± 4.8	29.3 ± 6.4	17.6 ± 5.6	53.2 ± 1.3
Smokers (N = 5)	35.2 ± 4.9	48.4 ± 6.2	11.1 ± 1.2	40.5 ± 8.3

* Values are expressed as percent ±SE of all metabolites formed and remaining nicotine. Abbreviations: COT, cotinine; NNX, nicotine-1′-*N*-oxide; and NIC, nicotine.

† Significantly different from control value in nonsmokers ($P < 0.05$).

‡ Significantly different from corresponding control value ($P < 0.05$).

Table 2. Nicotine metabolism and induction in male and female rats as reflected in hepatocytes*

	Males				Females			
	COT	NNC	NNX	NIC	COT	NNC	NNX	NIC
Control	15.9 ± 1.7	10.0 ± 1.7	13.0 ± 0.9	61.2 ± 2.4	14.0 ± 0.9	7.5 ± 2.1	12.2 ± 3.2	66.2 ± 4.8
β-Naphthoflavone	23.2 ± 5.5	19.0 ± 3.8†	27.6 ± 8.7†	30.2 ± 7.4‡				
Aroclor 1254	32.9 ± 4.8‡	19.4 ± 3.8†	23.5 ± 8.9	24.1 ± 3.6‡				
Phenobarbital	40.4 ± 3.7‡	27.7 ± 2.4‡	15.9 ± 1.3	15.9 ± 3.0§	27.1 ± 3.6§	18.1 ± 1.9§	18.2 ± 1.8	36.6 ± 4.5‡

* Values are expressed as percent ± SE of all metabolites formed and remaining nicotine; N = 6 for each sex in each of the three treatment groups as well as the control group. Abbreviations: COT, cotinine; NNC, nornicotine; NNX, nicotine-1′-*N*-oxide; and NIC, nicotine.

† $0.01 < P < 0.05$.

‡ $P < 0.001$.

§ $0.001 < P < 0.01$.

Table 3. Nicotine metabolism and induction in hamsters, guinea pigs and mice as reflected in hepatocytes*

	Hamster							Guinea pig					Mouse					
	ADC†	CNX	3HC	COT	NNC	NNX	NIC	3HC	COT	NNC	NNX	NIC	ADC	3HC	COT	NNC	NNX	NIC
Control	13.6 ± 0.8	13.6 ± 1.1	26.9 ± 2.4	18.0 ± 2.2	12.6 ± 2.5	7.3 ± 1.9	7.2 ± 0.7	5.2 ± 2.6	34.9 ± 3.1	10.6 ± 1.0	43.4 ± 5.0	5.9 ± 1.8	8.4 ± 2.5		26.4 ± 7.8	10.3 ± 1.5	8.9 ± 0.5	44.3 ± 12.5
β-Naphthoflavone	16.6 ± 3.1	10.4 ± 2.2	26.5 ± 3.9	21.6 ± 4.6	11.6 ± 2.2	6.9 ± 0.8	6.3 ± 1.0	10.8 ± 3.3	33.5 ± 3.9	16.1 ± 3.2	35.1 ± 7.8	4.5 ± 2.6	10.1 ± 2.5	11.5 ± 3.3‡	36.7 ± 7.7	12.1 ± 1.5	12.8 ± 0.6‡	16.1 ± 5.4‡
Phenobarbital	18.8 ± 3.2	16.5 ± 3.3	28.9 ± 3.3	14.2 ± 1.9	11.3 ± 1.4	4.9 ± 1.7	5.8 ± 1.7	15.7 ± 1.4‡	43.9 ± 1.7‡	13.1 ± 0.2‡	24.1 ± 0.5‡	3.1 ± 0.5	15.2 ± 2.9	13.0 ± 1.6§	45.8 ± 4.9‡	13.6 ± 3.0	9.2 ± 0.6	3.2 ± 1.2‡

* Values are expressed as percent ± SE of all metabolites formed and remaining nicotine; N = 6 for each species in each treatment group as well as each control group.

† Abbreviations: ADC, allohydroxydemethylcotinine; CNX, cotinine-*N*-oxide; 3HC, 3-hydroxycotinine; COT, cotinine; NNC, nornicotine; NNX, nicotine-1′-*N*-oxide; and NIC, nicotine.

‡ $0.01 < P < 0.05$.

§ $0.001 < P < 0.01$.

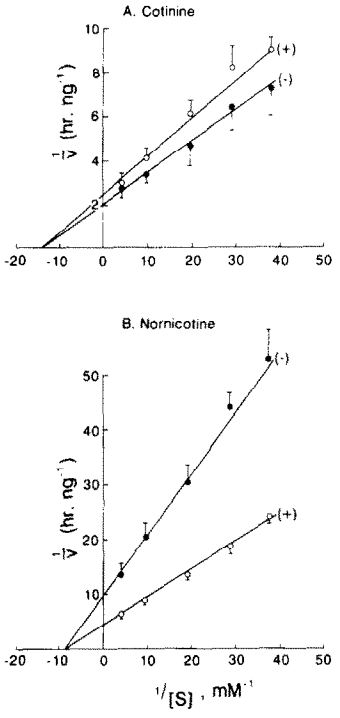

Fig. 5. Lineweaver–Burk reciprocal plots of the stereoselective metabolism by hamster hepatocytes of *R*-(+)- and *S*-(−)-nicotine to (A) cotinine and (B) nornicotine. Reaction mixtures consisted of: various concentrations of unlabeled-*R*-(+)- and *S*-(−)-nicotine; Tris–KCl (pH 7.4), 100 mM; NADPH, 0.5 mM; hepatocyte suspension, containing 2.5×10^6 cells. Values are means ± SE, N = 6.

Species variations in nicotine metabolism were demonstrated recently *in vivo* [2]. In hepatocytes, species variation ranged 3-fold, from virtually complete metabolism of nicotine (95%) by guinea pig hepatocytes to only 30% metabolism of nicotine by hepatocytes from rats and humans (Fig. 4). Marked species variations in the quantitative metabolism of nicotine *in vitro* have been reported by Jenner and coworkers [24, 25] using fortified 10,000 *g* hepatic supernatant fractions. They describe an order among species in nicotine-metabolizing capacity similar to that we observed in hepatocytes: guinea pig > hamster > mouse > rat (Fig. 4).

In *in vivo* studies of nicotine metabolism, 3′-hydroxycotinine has been reported to be the major urinary metabolite in hamsters, guinea pigs and humans [2, 26]. While this was true in the present study with hamster hepatocytes, the major nicotine metabolites produced by guinea pig and human hepatocytes were cotinine and nicotine-1′-*N*-oxide (Fig. 4; Tables 1 and 3).

Among human subjects, hepatocytes from cigarette smokers demonstrated induction of nicotine metabolism compared to hepatocytes from nonsmokers (Table 1). Also, hepatocytes of exsmokers exhibited a trend toward induction (Table 1). These observations support our previous conclusion [9] and that of others [27, 28] showing acceleration of nicotine and cotinine metabolism in smokers, as demonstrated by shorter plasma nicotine and cotinine terminal half-lives in smokers compared to nonsmokers. Induced nicotine metabolism in smokers has been questioned [29, 30].

Our results indicated that phenobarbital pretreatment also significantly induced nicotine metabolism in hepatocytes not only from humans (Table 1) but also from rats, guinea pigs, and mice (Tables 2 and 3). These results confirm earlier observations of induction of nicotine metabolism by phenobarbital pretreatment of guinea pigs [5] and rats [7]. The report of a 2-fold induction of 5′-hydroxylation of nicotine in hamsters pretreated with phenobarbital [6] was not reflected in increased production of cotinine in our present studies with hamster hepatocytes, perhaps because cotinine was further biotransformed to other metabolites. Lack of an effect of phenobarbital pretreatment on nicotine-1′-*N*-oxide production [6, 9] was confirmed in the present study for humans, rats and hamsters. The paradoxical inhibition of nicotine-1′-*N*-oxide production by phenobarbital observed with guinea pig hepatocytes (Table 3) was demonstrated previously in rabbit microsomes [31].

Sex differences in nicotine metabolism by hepatocytes from unmedicated rats did not reach statistical significance. Upon phenobarbital pretreatment, however, a highly significant sex difference (Table 2) occurred in the previously observed direction (male > females) [1].

Reasons for the large species and sex-dependent variations in nicotine metabolism and induction by phenobarbital, β-naphthoflavone and Aroclor warrant further investigation. In the various species we studied, different molecular forms of the hepatic enzymes involved in nicotine metabolism may occur constitutively, as well as after induction [31, 32]. Differential induction of these isozymes observed with the various inducing agents used in this study could provide one approach to unraveling the species-dependent heterogeneity of enzymes involved in nicotine metabolism.

Finally, hepatocytes revealed another aspect of nicotine metabolism: stereoselectivity. Hamster hepatocytes converted (*S*)-(−)-nicotine faster than (*R*)-(+)-nicotine to cotinine. The reverse occurred with metabolism of nicotine to nornicotine (Fig. 5). Such stereoselective differences in nicotine metabolism have been reported previously *in vitro* [11, 24], as well as *in vivo* [2, 3]. The nonradiometric assay used to demonstrate stereoselective metabolism of nicotine limited us to monitoring only its biotransformation to cotinine and nornicotine.

In conclusion, these results demonstrated species and sex differences, smoking-induced changes, selective induction of separate pathways and stereoselectivity for nicotine metabolism by hepatocytes. These applications of hepatocytes to investigate nicotine metabolism follow earlier studies on the metabolism of other drugs by hepatocytes [15–17, 33–38].

REFERENCES

1. Kyerematen GA, Owens GF, Chattopadhyay B, deBethizy JD and Vesell ES, Sexual dimorphism of nicotine

metabolism and distribution in the rat. *Drug Metab Dispos* **16**: 823–828, 1988.
2. Nwosu CG and Crooks PA, Species variation and stereoselectivity in the metabolism of nicotine enantiomers. *Xenobiotica* **18**: 1361–1372, 1988.
3. Jacob P, Benowitz NL, Copeland JR, Rimer ME and Cone EJ, Disposition kinetics of nicotine and cotinine enantiomers in rabbits and beagle dogs. *J Pharm Sci* **77**: 396–400, 1988.
4. Benowitz NL and Jacob P, Daily intake of nicotine during cigarette smoking. *Clin Pharmacol Ther* **35**: 499–504, 1984.
5. Nakayama H, Nakashima T and Kurogochi Y, Cytochrome P-450-dependent nicotine oxidation by liver microsomes of guinea pigs. Immunochemical evidence with antibody against phenobarbital-inducible cytochrome P-450. *Biochem Pharmacol* **34**: 2281–2286, 1985.
6. McCoy GD and deMarco GJ, Characterization of hamster liver nicotine metabolism. Differential effects of ethanol or phenobarbital pretreatment on microsomal N and C oxidation. *Biochem Pharmacol* **35**: 4590–4592, 1986.
7. Rudell U, Foth H and Kahl GF, Eightfold induction of nicotine elimination in perfused rat liver by pretreatment with phenobarbital. *Biochem Biophys Res Commun* **148**: 192–198, 1987.
8. Nwosu CA, Godin CS, Houdi AA, Damani LA and Crooks PA, Enantioselective metabolism during continuous administration of *S*-(−)- *and R*-(+)-nicotine isomers in the guinea pig. *J Pharm Pharmacol* **40**: 862–869, 1988.
9. Kyeremeten GA, Damiano MD, Dvorchik B and Vesell ES, Smoking-induced changes in nicotine disposition: Application of a new HPLC assay for nicotine and its metabolites. *Clin Pharmacol Ther* **32**: 769–780, 1982.
10. Stalhandske T, The metabolism of nicotine and cotinine by a mouse liver preparation. *Acta Physiol Scand* **78**: 236–248, 1970.
11. Jenner P, Gorrod JW and Beckett AH, Factors affecting the *in vitro* metabolism of *R*-(+)- and *S*-(+)-nicotine by guinea pig liver preparations. *Xenobiotica* **3**: 563–572, 1973.
12. Hansson E, Hoffman PC and Schmitterlow CG, Metabolism of nicotine in mouse tissue slices. *Acta Physiol Scand* **61**: 380–392, 1964.
13. Stalhandske T, Slanina P, Tjalve H, Hansson E and Schmitterlow CG, Metabolism *in vitro* of ^{14}C-nicotine in livers of fetal, newborn and young mice. *Acta Pharmacol Toxicol* **27**: 363–380, 1969.
14. Abood LG, Grassi S, Junig J, Crane A and Contanzo M, Specific binding and metabolism of (−)- and (+)-[^{3}H]-nicotine in isolated rat hepatocytes and hepatocyte membranes. *Arch Int Pharmacodyn Ther* **273**: 62–73, 1985.
15. Chenery RJ, Ayrton A, Oldham HG, Standing P, Normal SJ, Seddon T and Kirby R, Diazepam metabolism in cultured hepatocytes from rat, rabbit, dog, guinea pig and man. *Drug Metab Dispos* **15**: 312–317, 1987.
16. Berthou F, Ratanasavanh D, Riche C, Picart D, Voirin T and Guillouzo A, Comparison of caffeine metabolism by slices, microsomes and hepatocyte cultures from adult human liver. *Xenobiotica* **19**: 401–417, 1989.
17. LeBigot JF, Bejee JM, Kiechel JR and Guillouzo A, Species differences in metabolism of ketotifen in rat, rabbit and man: Demonstration of similar pathways *in vivo* and in cultured hepatocytes. *Life Sci* **40**: 883–890, 1987.
18. Kyerematen GA, Taylor LH, deBethizy JD and Vesell ES, Radiometric-high performance liquid chromatographic assay for nicotine and twelve of its metabolites. *J Chromatogr* **419**: 191–203, 1987.
19. Wang SR, Renaud G, Infante J, Catala D and Infante R, Isolation of rat hepatocytes with EDTA and their metabolic functions in primary culture. *In Vitro Cell Dev Biol* **21**: 526–529, 1985.
20. Moldeus P and Orrenius S, Isolation and use of liver cells. *Methods Enzymol* **52**: 60–71, 1978.
21. Strom SC, Jirtle RL, Jones RS, Novicki DL, Rosenberg MR, Novotny A, Irons G, McLain JR and Michalopoulos G, Isolation, culture and transplantation of human hepatocytes. *J Natl Cancer Inst* **68**: 771–778, 1982.
22. Sitar DS, Human drug metabolism *in vivo*. *Pharmacol Ther* **43**: 363–375, 1989.
23. McCoy GD, Howard PC and deMarco GJ, Characterization of hamster liver nicotine metabolism. Relative rates of microsomal C and N oxidation. *Biochem Pharmacol* **35**: 2767–2773, 1986.
24. Jenner P, Gorrod JW and Beckett AH, Species variation in the metabolism of *R*-(+)- and *S*-(−)-nicotine by α-C and N-oxidation *in vitro*. *Xenobiotica* **3**: 573–580, 1973.
25. Jenner P and Gorrod JW, Comparative *in vitro* hepatic metabolism of some tertiary *N*-methyl tobacco alkaloids in various species. *Res Commun Chem Pathol Pharmacol* **6**: 829–843, 1973.
26. Neurath GB, Dusinger M, Orth D and Pein FG, Trans-3′-hydroxycotinine as a main metabolite in urine of smokers. *Int Arch Occup Environ Health* **59**: 199–201, 1987.
27. Sepkovic DW, Haley NJ and Hoffmann D, Elimination from the body of tobacco products by smokers and passive smokers. *JAMA* **256**: 863, 1986.
28. Etzel RA, Greenberg RA, Haley NJ and Loda FA, Urinary cotinine excretion in neonates exposed to tobacco smoke products *in utero*. *J Pediatr* **107**: 146–148, 1985.
29. Jarvis MJ, Russell MAH, Benowitz NL and Feyerabend C, Elimination of cotinine from body fluids: Implications for noninvasive measurement of tobacco smoke exposure. *Am J Public Health* **78**: 696–698, 1988.
30. Barlow RD and Wald NJ, Use of urinary cotinine to estimate exposure to tobacco smoke. *JAMA* **259**: 1808, 1988.
31. McCoy GD, deMarco GJ and Koop DR, Microsomal nicotine metabolism: A comparison of relative activities of six purified rabbit cytochrome P-450 isozymes. *Biochem Pharmacol* **38**: 1185–1188, 1989.
32. Nakayama H, Nakashima T and Kurogochi Y, Heterogeneity of hepatic nicotine oxidase. *Biochim Biophys Acta* **715**: 254–257, 1982.
33. Loft S and Poulsen HE, Metabolism of metronidazole and antipyrine in isolated rat hepatocytes. *Biochem Pharmacol* **38**: 1125–1136, 1989.
34. Ohno Y, Najamatsu K, Kawanishi T, Ikebuchi H, Terao T and Takanaka A, Comparative evaluation of different pathways for the liver toxicity of morphine using freshly isolated hepatocytes. *Biochem Pharmacol* **37**: 2862–2863, 1988.
35. McCormick DJ, Fitzgerald TC and McKillop D, The metabolism of propranolol (ICI 45,520, Inderal™) and xamoterol (ICI 118,587, Corwin™) by isolated rat hepatocytes: *In vivo–in vitro* correlations. *Xenobiotica* **18**: 1401–1412, 1988.
36. Hempel M, Sastarek D, Giescher H and Lobitzky C, Studies on the biotransformation of lonazolac, bromerguride, lisuride and terguride in laboratory animals and their hepatocytes. *Xenobiotica* **19**: 361–377, 1989.
37. Fabre G, Rahmani R, Placidi M, Combalbert J, Covo J, Cano J-P, Coulange C, Ducros M and Rampal M, Characterization of midazolam metabolism using

human hepatic microsomal fractions and hepatocytes in suspension obtained by perfusing whole human livers. *Biochem Pharmacol* **37**: 4389–4397, 1988.

38. Chiba M, Fujita S and Suzuki T, Kinetic properties of the metabolism of imipramine and desimipramine in isolated rat hepatocytes. *Biochem Pharmacol* **39**: 367–372, 1990.